JOURNAL OF MATERIALS SCIENCE 23 (1988) 1825–1828

Spallation as an effect of laser-induced shock waves

IRITH GILATH, DAVID SALZMANN, MEIR GIVON
Plasma Physics Department, Soreq Nuclear Research Centre, Yavne 70600, Israel
MOSHE DARIEL*, LEVI KORNBLIT
Material Science Department, Ben Gurion University, Beer Sheva, Israel
TUVIA BAR-NOY
**Physics Department, Nuclear Research Centre, Negev, POB 9001, Beer Sheva 84190, Israel*

Spallation resulting from laser-driven shock waves in metallic foils was investigated and the various stages of material failure were identified. The very high strain rate ($10^7 sec^{-1}$) characteristic of these experiments sets our results apart from those obtained by high explosives or hypervelocity impact. Numerical hydrodynamic simulations of the phenomenon were developed and are shown to be in qualitative agreement with the experimental results.

1. Introduction

Research into spallation and dynamic fracture phenomena has lately found application in several fields such as projectile damage in a variety of targets, spacecraft design and re-entry related problems. The general interest in spallation phenomena is also linked to the determination of damage threshold criteria in materials subjected to propagation of intense shock waves produced by projectile impact, explosions or irradiation by intense laser beams.

The term spallation in the context of shock wave research is defined as the separation of material along a plane parallel to the wave front, and resulting from the development of dynamic tensile stress components perpendicular to this plane [1, 2]. Spallation in ductile materials is controlled by localized plastic deformations along small voids which grow and coalesce to form the spall plane [3]. In brittle materials, spallation takes place by dynamic crack propagation with no accompanying plastic deformation.

Conventional techniques for the study of spallation effects include the plate impact method and the use of high explosives. Recently, laser-induced shock waves have also been applied for studying spallation effects [4] and changes in the metal microstructure [5]. The apparent advantage of the latter method lies in its associated strain rates of the order of $10^7 sec^{-1}$ and above, as compared to strain rates of $10^6 sec^{-1}$ at most, obtainable by the other techniques. The extremely high strain rate opens a new domain for the investigation of the mechanical behaviour of various materials under ultrafast dynamic conditions.

Other advantages of the use of lasers for the study of spallation phenomena are the minute quantity of materal involved and the improved control of the experimental conditions, for example the possibility of efficiently collecting the ejected material.

The objective of the present work was to understand the behaviour of metallic material under high pressure and high strain rate generated by a laser-induced shock wave, and to study the resulting stages of material failure such as internal crack formation, spallation and target perforation. In particular, we describe the determination of the energy threshold required to induce the various stages of the spalling phenomena.

2. Scientific background

Absorption of laser radiation by a target material takes place within a very thin layer, about 1 μm thick, near the irradiated surface. The rapid temperature increase in this layer ($10^3 eV\,nsec^{-1}$) and the associated steep temperature gradient ($10^7 eV\,cm^{-1}$) induce ablation of the plasma material into the vacuum. This expansion drives a strong shock wave in the opposite direction, into the cold substrate, thereby compressing it to high densities. The shock wave pressure, P, is directly related to the laser pulse intensity, I, scaling approximately as $P = I^{3/4}$, in a manner almost independent of the nature of the material. Typically, a 1.3 Mbar pressure is obtained for an irradiation level of $I = 10^{13} W\,cm^{-2}$ in an aluminium slab target. The accurate values of the shock pressure can be calculated by hydrodynamic simulation. Two-dimensional simulations verified by experimental results show that the shock wave is fairly planar as long as the focal spot radius is larger than the target foil thickness. The shock wave profile is rectangular as long as the laser pulse is on, later a rarefaction wave from the front (laser irradiated side) takes over and a compression wave with a triangular profile develops. This triangular wave profile is essential for spallation phenomena to develop [6, 7]. As the triangular-shaped compression wave reaches the back surface, a tensile wave of increasing negative amplitude is reflected from the free surface back into the sample. When the tensile stress becomes larger than the tensile strength of the target, spallation occurs.

0022–2461/88 $03.00 + .12

3. Experimental method

The Nd : glass laser at the Plasma Physics Laboratory at the Soreq Research Centre has been designed for single beam high irradiance, 1.06 μm wavelength interaction studies.

A cavity-dumped Q-switched oscillator was constructed in order to generate temporally shaped laser pulses in the nanosecond domain. The performance of the system was demonstrated through the generation of flat-topped step pulses having a rise-time of 0.2 nsec and controllable duration of 1 to 7 nsec. This trapezoidal pulse shape [8] is optimal for shock wave generation.

The successive amplifier stages deliver up to 80 J energy. In the course of the experiments, the focal spots were varied between 0.25 and 2 mm, in order to ensure planar shock wave propagation. The corresponding pulse intensities were 10^{11} to 10^{13} W cm^{-2}, resulting in shock wave pressures of the order of 0.1 Mbar in the target metals. The system repetition rate was 30 min and the output energy was stable within 2%.

Optical and scanning electron microscopy were used for examining the damage caused by the laser pulse irradiation and metallurgical sectioning was used for internal damage evaluation. Optical and scanning electron microscopy can be used for the characterization of the brittle or ductile dynamic fracture and for the measurement of crater depth and diameter. Metallurgical sectioning reveals the internal damage and the thickness of the spalled layer.

4. Experimental results

The various stages of the target material failure that were observed with increasing laser pulse intensity are shown schematically in Fig. 1. For very low intensities, no damage is observed on the back surface of the target while a shallow crater due to ablation of material at the point of impact of the laser beam becomes visible (Fig. 1a). With increasing pulse intensity, the target spalls, i.e. an internal crack develops causing a swelling on the back surface (Fig. 1b). At still higher intensities, the material beyond the spalled plane is severed from the bulk of the target, leaving a crater on its rear surface (Fig. 1c). The crater depth increases with increasing pulse power until the back and front side craters meet and target perforation occurs (Fig. 1d).

The experimentally observed counterparts of these phenomena are shown in the following figures. The initial material failure appears as a swelling on the back surface, similar for brittle or ductile materials (Fig. 2). By metallurgical sectioning, the brittle material revealed parallel spallation planes which may have been

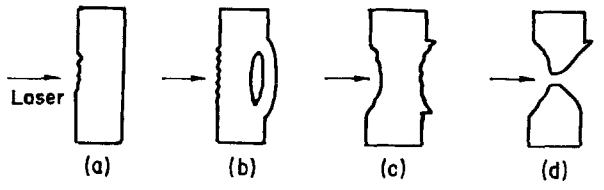

Figure 1 Stages of material failure.

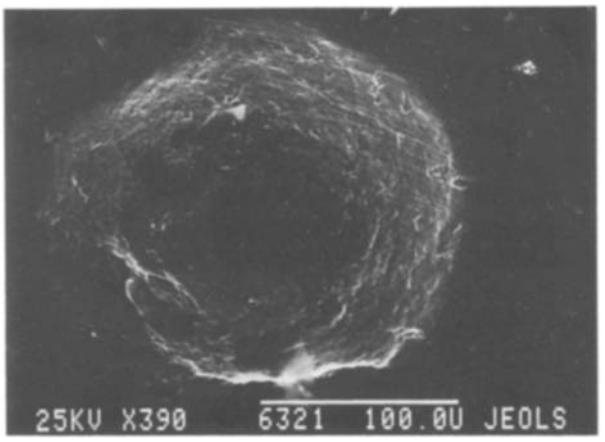

Figure 2 Swelling of the back surface.

caused by shock reverberation (Fig. 3). In annealed aluminium, only one spall plane was observed (Fig. 4). For higher irradiation intensities, the material beyond the spall plane splits open, yet the lid stays connected to the target (Fig. 5). The metallurgical sectioning of this sample is shown in Fig. 6. For still higher laser pulse intensities, a complete perforation of an aluminium target occurs as shown in Fig. 7.

5. Computer simulation

The theoretical simulation of the phenomena discussed in this work involves the simultaneous solution of the three conservation equations (of mass, momentum and energy) along with the equation of state (EOS) of the material under consideration. As long as one deals with thin foils with the size of the laser spot larger than the foil thickness, one can employ a one-dimensional computer code. The code that was used is the two-temperature MEDUSA code [9]. The code involves the finite-difference equations in Lagrangian coordinates for slab, cylindrical or spherical geometry. Part of the laser light is absorbed via inverse brehmstrahlung (in the under-dense plasma), while the remaining fraction is absorbed in the critical density cell. The absorbed energy is transferred into the foil by thermal conduction. The EOS were taken from the SESAME library [10]. Elastic stresses are not included because the inelastic shock waves produced by the intense laser pulse tend to shade the (small) elastic wave. The mechanism of spall formation was introduced through a single parameter, namely the material tensile strength criterion. This parameter can be varied

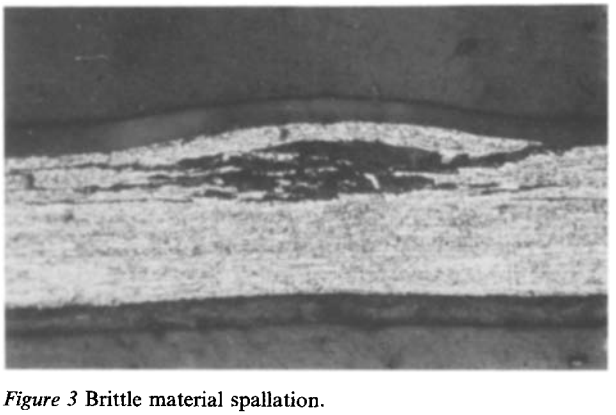

Figure 3 Brittle material spallation.

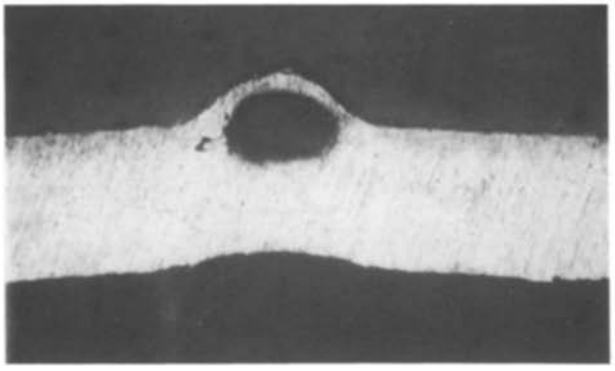

Figure 4 Ductile material spallation.

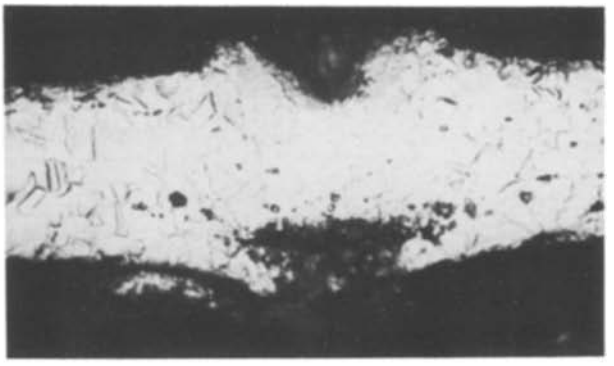

Figure 6 Metallurgical sectioning.

and was chosen to be -30 kbar [11, 12, 13]. Each numerical cell is "spalled" when the associated pressure attains a value more negative than -30 kbar. After spallation, the pressure of the cell is kept zero while its energy and mass are conserved. This rather simple formulation of the spall criterion is justified *a posteriori* by the good agreement with the experimental results.

The laser pulse had a trapezoidal shape, corresponding to the actual experimental pulse shape, with a rise-time of 0.4 nsec and a duration of 4.3 nsec. The power level was changed to simulate the different experiments. The aluminium foil target was divided into a finite number of zones in a way that ensured numerical convergence. Convergence was checked by showing the insensitivity of the results to further refining of the numerical mesh.

The shock wave produced in the 100 μm wide aluminium foil target reaches its rear end in about 10 to 15 nsec (depending on the power level of the laser pulse). After being reflected from the back surface, the (negative) stress wave will cause spallation in the target if its amplitude is greater than the tensile strength. After about 20 to 30 nsec, the shock waves are damped and the foil reaches its final state with further changes being negligible. Figs 8 to 10 show the density–distance behaviour resulting from three laser pulses of different power levels; at $t = 15$ nsec, the shock wave does not reach the back surface for the $I = 0.63 \times 10^{11}$ W cm^{-2} pulse (Fig. 8), it just starts being reflected for the $I = 2.37 \times 10^{11}$ W cm^{-2} pulse (Fig. 9) and has already caused a spall for the highest intensity laser pulse of $I = 11.8 \times 10^{11}$ W cm^{-2} (Fig. 10). At $t = 30$ nsec, the three cases display a similar behaviour. Region (a) is the back surface of the foil containing the material beyond the spall plane. The width of this region varies with the laser power. Region (b) is the void, that is the spalled zone in which, actually, several spall planes can be distinguished. Region (c) is the solid part of the slab that remains after the shock wave has been damped, its width is 80, 60 and 25 μm for the three cases. Finally region (d) represents the plasma blow-off of the front surface of the target foil and is about 10 to 20 μm wide.

Comparing Figs 8 to 10, the simulation results, with the experimental ones shown in Figs 3 to 7, we should bear in mind the two-dimensional effects in the target foil. As a result of the finite radial extension of the pressure-affected zone, if its velocity is small, the back surface is held back by its edges and is prevented from running away to the left. Thus, for the lowest intensity case, the material beyond the spalled plane, region (a) remains connected to the foil at its edges, yet the void created within the foil is clearly apparent both in the experimental cross-section (Figs 3 and 4) and in the numerical simulation (Fig. 8). For the two higher intensity cases the spalled back-surface region is split off the foil to the left, leaving behind craters 40 and 60 μm deep, respectively. Particularly noteworthy is the result of the highest intensity case. In this case, region (c), the main part of the target foil, between the ablated front crater and the spalled off back crater, reaches a lower density than that of solid metal. This implies that the bulk of the target material has evaporated, and the foil is perforated as actually can be observed in Figs 7 (experimental) and 10 (simulation).

Thus, the 1D simulation accounts for most of the experimental observations, including the spall, the formation of the front and back craters, their

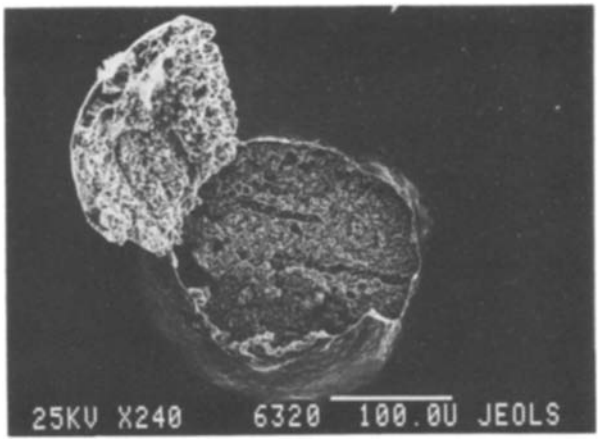

Figure 5 Crater opening.

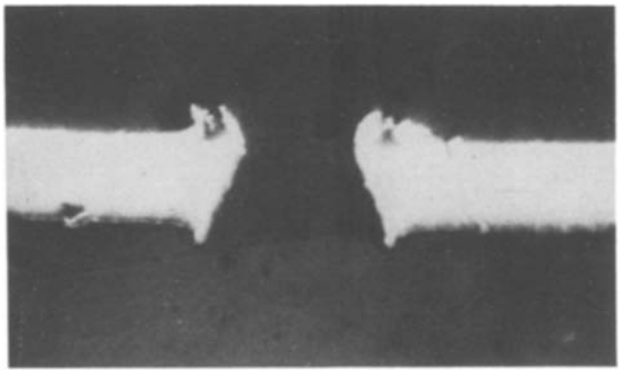

Figure 7 Complete perforation of target.

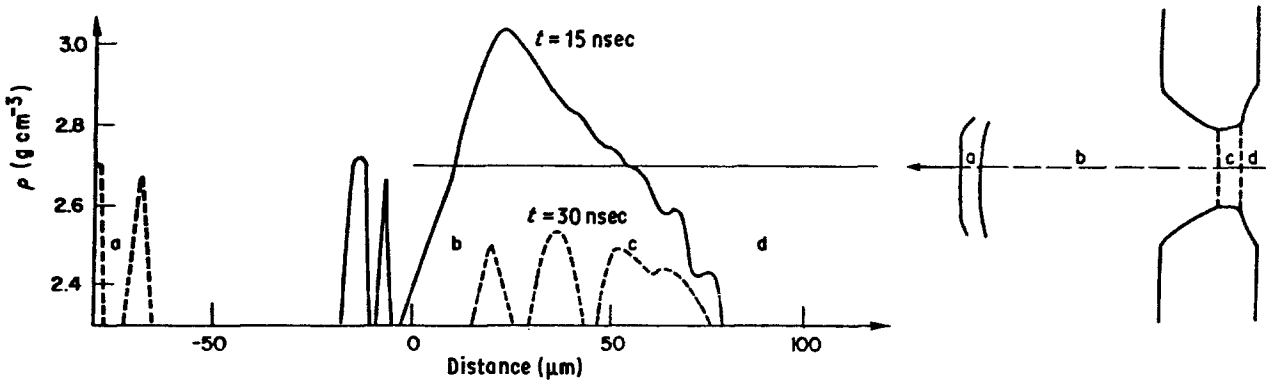

Figure 8 Density plotted against distance for aluminium irradiated at $I = 0.63 \times 10^{11}\,\mathrm{W\,cm^{-2}}$.

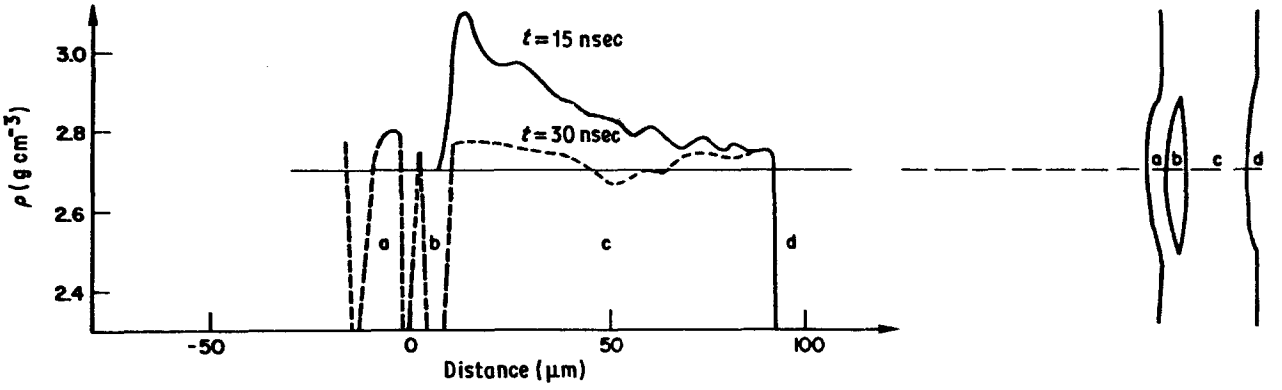

Figure 9 Density plotted against distance for aluminium irradiated at $I = 2.37 \times 10^{11}\,\mathrm{W\,cm^{-2}}$.

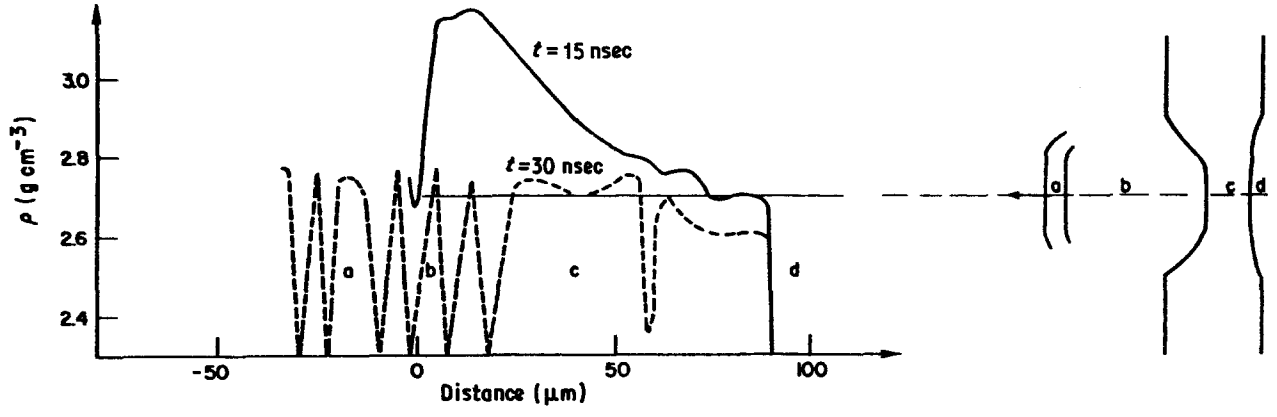

Figure 10 Density plotted against distance for aluminium irradiated at $I = 11.8 \times 10^{11}\,\mathrm{W\,cm^{-2}}$.

respective depth, and the perforation of the target foil for the high-intensity cases.

Acknowledgements

The authors thank the Plasma Physics Group for help in carrying out the experiments. Mr Y. Sapir's technical assistance is greatly appreciated.

References

1. J. N. JOHNSON, *J. Appl. Phys.* **52** (1981) 2812.
2. T. W. BARBEE, L. SEAMAN, R. CREWDSON and D. CURRAN, *J. Mater.* **7** (1972) 393.
3. D. R. CURRAN, D. A. SHOCKEY and L. SEAMAN, *J. Appl. Phys.* **44** (1973) 4025.
4. C. G. HOFFMANN, "Some effects of laser irradiation on aluminium", Los Alamos Scientific Laboratory Report, LA-6189-MS, Apr. 1976.
5. A. H. CLAUER, J. H. HOLBROK and B. FAIRAND, in "Shock Waves and High Strain Rate Phenomena in Metals" edited by M. A. Meyers and L. E. Murr (Plenum, New York, 1980) Ch. 38.
6. YA. B. ZELDOVITCH and YU. P. REISER, "Physics of shock waves and high temperature hydrodynamic phenomena" (Academic, New York, 1967).
7. J. ZUCKAS, T. NICHOLAS, M. SWIFT, L. GRESZCZUK and D. CURRAN, "Impact Dynamics" (Wiley, New York, 1982).
8. B. ARAD, A. BOROWITZ, S. ELIEZER, Y. GAZIT, I. GILATH, M. GIVON, S. JACKEL, A. KRUMBEIN and H. SEICHMANN, *Plasma Phys. Controlled Fusion* **26** (1984) 845.
9. D. E. T. F. ASHBY, J. P. CHRISTIANSEN and K. V. ROBERTS, *Computer Phys. Commun.* **7** (1974) 271.
10. B. I. BENNET, J. D. JOHNSON, G. I. KERLEY and G. T. ROAD, Los Alamos Lab. Report LA 7130 (1978).
11. J. S. RINEHART, *J. Appl. Phys.* **22** (1951) 555.
12. J. L. O'BRIEN, Harvard Univ. Doc. 35-61-12 (1961).
13. B. R. BREED, *et al.*, *J. Appl. Phys.* **38** (1967) 3271.

Received 2 April
and accepted 16 June 1987